Bull. Inst. Chem. Res., Kyoto Univ., Vol. 57, No. 2, 1979

# Time-Dependent Flow Fields in a Coaxial Cylinder Rheometer. The Flow of a BKZ Fluid at the Start of Rotation

Kunihiro OSAKI, Kanji KAJIWARA, Nobuo BESSHO†, and Michio KURATA*

*Received March 7, 1979*

Numerical calculations were performed to study the flow of polymeric liquids at the start of rotation of a coaxial cylinder rheometer. The rheological behavior of polymeric liquids was assumed to be represented by a strain-dependent constitutive model of Bernstein, Kearsley, and Zapas (BKZ model) and the stress equation of motion was solved with an electronic computer. The distribution of rate of shear starts from that expected for the steady flow of a Newtonian liquid and approaches the distribution obtained for the steady flow of a power law liquid. The rate of shear at a fixed point varies monotonously at low rates of rotation where the phenomenon of stress-overshoot is not very marked. At high rates of rotation, the rate of shear passes over a maximum or a minimum, respectively, depending on whether the sample is located close to the inner wall or the outer wall. At a certain radius slightly smaller than the average of the inner and outer radii of the cylindrical gap, the rate of shear scarcely depends on time provided that the rotation velocity and the gap width are not too large. The use of coaxial cylinder rheometer to measure time-dependent shear stresses is justified under the same condition.

KEY WORDS: Coaxial cylinder rheometer/ Polymer solution/ Non-Newtonian viscosity/ BKZ/ Constitutive model/

## INTRODUCTION

The Couette flow, which is one of the important rheometrical flows, is the flow of the liquid in the narrow gap of two coaxially placed cylinders in relative rotation as shown in Fig. 1. The coaxial cylinder rheometer based on the Couette flow exhibits some advantages over other rheometers such as the cone-and-plate rheometer; liquids of even low viscosities can be held in the cylindrical gap; high rates of shear can be attained without any out-flow of the sample due to the centrifugal force; the cylindrical gap affords a simple and long light pass for optical studies in flow field such as the flow birefringence measurement.

On the other hand, the Couette flow has a disadvantage as a rheometrical flow in that the flow field is uncontrollable,[1] *i.e.*, the velocity distribution is not determined by the relative rotation velocity of the cylinders alone but it also depends on the rheological property of the liquid. In the studies of rheological properties of liquids, it is desirable to apply to the liquid a rate of shear $\dot{\gamma}$ of a value known beforehand. The rate of shear is related to the velocity $v$ by

* 尾崎邦宏，梶原莞爾，別所信夫，倉田道夫：Laboratory of Polymer Physical Chemistry, Institute for Chemical Research, Kyoto University, Uji, Kyoto.

† Present Address: Central Research Laboratory, Japan Synthetic Rubber Co., Ltd., 7569 Ikuta, Kawasaki, Kanagawa 214.

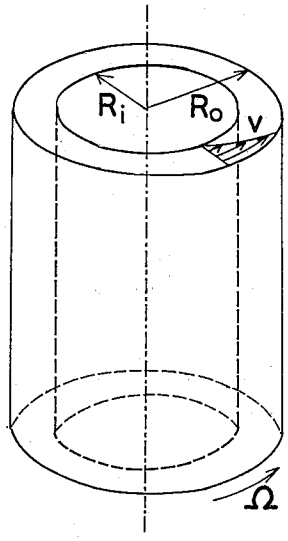


Fig. 1. Coaxial cylinder apparatus. Test liquid is confined within cylindrical gap formed by two coaxially placed cylinders of radii $R_i$ and $R_o$, respectively. Outer cylinder is rotated with angular velocity $\Omega$ while inner cylinder is kept stationary. Velocity profile $v$ depends not only on $R_i$, $R_o$, and $\Omega$, but on properties of test liquid.

$$\dot{\gamma} = r\frac{\partial}{\partial r}\left(\frac{v}{r}\right) \tag{1}$$

in the case of the Couette flow in a cylindrical gap. For a Newtonian liquid in steady flow, the rate of shear at a point $r$ is given by

$$\dot{\gamma} = \frac{2\Omega}{r^2(R_i^{-2}-R_o^{-2})} \tag{2}$$

where $R_i$ and $R_o$ are respectively the radii of the inner and the outer surfaces of the cylindrical gap and $r$ denotes the distance of the point from the axis. The angular velocity at $r=R_o$ is taken as $\Omega$ and that at $r=R_i$ as 0. The viscosity of any Newtonian liquid can be evaluated by measuring the torque exerted by the liquid on the inner cylinder since the rate of shear on the surface of the inner cylinder can be calculated from Eq. (2).

When the viscosity varies with the rate of shear, Eq. (2) is not applicable. For a power-law fluid described by

$$\eta \propto \dot{\gamma}^{n-1} \qquad (1 \geq n > 0) \tag{3}$$

the rate of shear in steady flow is given by

$$\dot{\gamma} = \frac{2\Omega}{nr^{2/n}(R_i^{-2/n}-R_o^{-2/n})} \tag{4}$$

where $n$ is a constant. In this case, one cannot evaluate the viscosity from the torque

exerted on the inner cylinder unless one knows the value of $n$, which belongs to the quantities to be determined through measurement. A widely employed procedure[2] to evaluate the rate of shear for non-Newtonian liquids consists of evaluating the approximate values of the rate of shear with Eq. (2), determining an approximate value of $n$ from the shear stress and the approximate rate of shear, and then recalculating the rate of shear with an equation corresponding to Eq. (4).

In the measurement of time-dependent rheological properties, such as the stresses at the start or on the cessation of shear flow, the stress varies from time to time. It is not always possible to apply a constant rate of shear. If the rheological property of the material is described by the linear viscoelasticity theory, Eq. (2) holds good in slowly varying flow, in which the inertial force is negligible compared with the force due to the stress. Thus Eq. (2) is applicable to ordinary viscoelastic materials, such as polymer solutions, when the rotation velocity $\Omega$ is small and changes slowly. In the special case of oscillatory shear, the rate of shear at the inner surface has been calculated over all the frequency range for linear viscoelastic materials.[3]

The time-dependent flow in the cylindrical gap of nonlinear materials is essentially uncontrollable even for a slowly varying flow. Equation (4) may be applied to slow flow of a purely viscous power-law liquid, which unfortunately is not even a fair model for existing nonlinear materials. Thus the rate of shear may vary with the time as well as with the position when a constant velocity $\Omega$ is applied to the outer cylinder. However, the rate of shear at the center of the cylindrical gap, *i.e.*, at $R_c \equiv (R_i+R_o)/2$, may stay rather constant as guessed from the comparison of Eqs. (2) and (4). If the rate of shear stays constant at least at one point, the coaxial cylinder system can be used for rheological measurements at the start of steady shear flow. The purpose of the present study is to calculate the flow field on application of constant rotation velocity $\Omega$ to the outer surface of the cylindrical gap based on a reasonable model to describe the rheological properties of concentrated polymer solutions.

## METHOD

### Basic Equations

The velocity of the liquid is determined from the stress equation of motion, the constitutive equation of the material, and the boundary condition. In the present case we may assume that the axial and the radial components of the velocity are zero, and that the velocity $v$ is a function of radius $r$ and time $t$. The stress equation of motion is given by

$$\rho \frac{\partial v}{\partial t} = \frac{1}{r^2} \frac{\partial (r^2 \sigma)}{\partial r} \tag{5}$$

where $\rho$ is the density of the liquid and $\sigma$ is the shear stress. The stress equation of motion may be replaced by the stress equation of equilibrium

$$\frac{\partial (r^2 \sigma)}{\partial r} = 0 \tag{6}$$

since we are concerned with a slowly varying process which is much slower than the stress-equilibrating process. To estimate the velocity of the stress-equilibrating process, we consider a unidirectional shear flow of a liquid of viscosity $\eta$ held between two parallel plates. The stress equation of motion is given by

$$\rho\frac{\partial v}{\partial t}=\frac{\partial \sigma}{\partial x} \tag{7}$$

where $x$ is the coordinate taken perpendicularly to the plates. Differentiating with respect to $x$, one obtains

$$\frac{\partial \sigma}{\partial t}=\frac{\eta}{\rho}\frac{\partial^2 \sigma}{\partial x^2} \tag{8}$$

According to this equation, a time $t_{eq}\equiv\rho l^2/2\eta$ is sufficient for the stress applied on one side of the liquid to diffuse over the whole liquid, where $l$ is the distance between the plates.[4] Suppose $\rho=1$ g/cm$^3$, $\eta=100$ Pa s, and $l=1$ mm, one obtains $t_{eq}=0.5$ ms. Thus for typical polymer solutions, the stress becomes homogeneous over the sample of 1 mm depth within 1 ms. For processes of longer time scales, like the present case as seen later, one can safely assume that the stress is equilibrated over the sample at each moment.

The boundary condition for the sudden start of constant rotation is given by

$$\begin{aligned} &v=0 \quad \text{at} \quad r=R_i \\ &\text{and} \\ &v=0 \qquad t<0 \\ &\quad r\Omega \qquad t\geq 0 \quad \text{at} \quad r=R_o \end{aligned} \tag{9}$$

Using Eq. (1), one can rewrite Eq. (9) as

$$\int_{R_i}^{R_o}\frac{\dot{r}}{r}\mathrm{d}r=\begin{cases} 0 & t<0 \\ \Omega & t\geq 0 \end{cases} \tag{10}$$

As a constitutive model to represent concentrated polymer solutions, we chose the strain-dependent model of Bernstein, Kearsely, and Zapas, or the BKZ model.[5] The model has proved good in describing the stresses at the start and on the cessation of steady shear flow.[6,8] According to this model, the shear stress in shear flow is given by

$$\sigma(t)=\int_{-\infty}^{t}\gamma(t,t')\mu[t-t',|\gamma(t,t')|]\mathrm{d}t' \tag{11}$$

where the relative shear strain $\gamma(t,t')$ is given by

$$\gamma(t,t')=\int_{t'}^{t}\dot{\gamma}(t'')\mathrm{d}t'' \tag{12}$$

The function $\mu$ is called the memory function and may be written as

$$\mu(t-t', \gamma) = \sum_p \frac{G_p h_p(\gamma)}{\tau_p} e^{-(t-t')/\tau_p} \tag{13}$$

in terms of the relaxation time $\tau_p$, relaxation strength $G_p$, and the strain-dependent function $h_p(\gamma)$ to represent the nonlinearity. The strain-dependent function $h_p(\gamma)$ can well be described as a sum of exponential functions for typical polymer solutions.[6,8] Here we assumed

$$h_p(\gamma) = e^{-\alpha\gamma} \tag{14}$$

with $\alpha=0.4$. The simple functional form and the specific value of $\alpha$ were suitable for describing the behavior of many polystyrene solutions.[6] Two sets of values of $G_p$ and $\tau_p$ were tested:

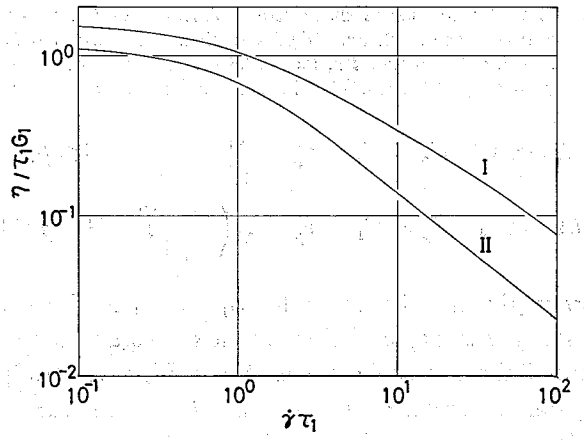


Fig. 2. Reduced steady shear viscosity $\eta/\tau_1 G_1$ plotted against reduced rate of shear $\dot{\gamma}\tau_1$ for two models employed for numerical calculations.

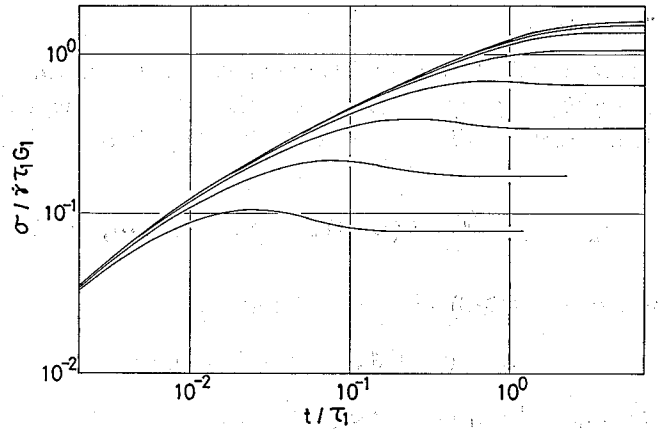


Fig. 3. Time dependence of shear stress following sudden application of constant rate of shear. Reduced shear stress $\sigma/\dot{\gamma}\tau_1 G_1$ is plotted against reduced time $t/\tau_1$ for model I. Reduced rates of shear $\dot{\gamma}\tau_1$ are 0, 0.1, 0.316, 1.0, 3.16, 10, 31.6, and 100 from top to bottom.

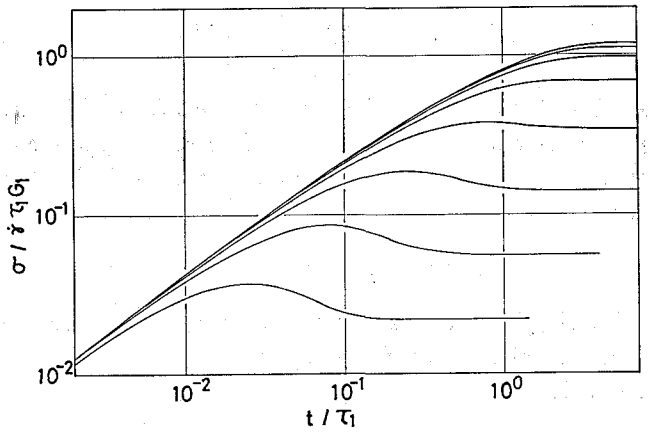


Fig. 4. Time dependence of shear stress following sudden application of constant rate of shear. Reduced shear stress $\sigma/\dot{\gamma}\tau_1 G_1$ is plotted against reduced time $t/\tau_1$ for model II. Reduced rates of shear $\dot{\gamma}\tau_1$ are 0, 0.1, 0.316, 1.0, 3.16, 10, 31.6, and 100 from top to bottom.

$$\text{Model I} \quad G_p = G_1 \quad \tau_p = \frac{\tau_1}{p^2} \qquad 1 \leq p \leq 20 \tag{15a}$$

$$\text{Model II} \quad G_p = G_1 \quad \tau_p = \tau_1 \left(\frac{2}{p+1}\right)^5 \qquad 1 \leq p \leq 10 \tag{15b}$$

It is not necessary to give definite values for $G_1$ and $\tau_1$ in the following. Figure 2 shows the steady shear viscosity $\eta$ of these models. Figures 3 and 4 show the shear stress $\delta$ at the start of shear flow for models I and II, respectively. It may be obvious that the model II represents a liquid which is nonlinear to a greater extent than the model I; for the model II the viscosity decreases more rapidly with the rate of shear and the stress overshoot, *i.e.*, the maximum of the shear stress $\sigma$, is more marked than for the model I.

**Calculation Procedure**

The procedure of calculation consists essentially of solving the set of Eqs. (6), (10), and (11) step by step by approximating the differential equation with a difference equation. First we divide the cylindrical gap into $M$ shells and choose $M+1$ points

$$r_m = R_i + \frac{R_o - R_i}{M}(m-1), \qquad m = 1, 2, \cdots, M+1 \tag{16}$$

We also divide the time ($t \geq 0$) in unit of $\Delta$ and denote

$$t_u = (u-1)\Delta, \qquad u = 1, 2, 3, \cdots \tag{17}$$

Any time between $t_u$ and $t_{u+1}$ may be expressed by

$$t = t_u + s\Delta \tag{18}$$

where $s$ varies from zero to unity.

The basic assumptions involved in the following calculation are that the rate of shear is constant over each $\Delta$ period and that the difference of the rate of shear between neighboring $\Delta$ periods of time is much smaller than $1/\tau_1$. We define a strain at time $t_u$ relative to the time zero by

$$g_{um} = \int_0^{t_u} \dot{\gamma}_m(t')\mathrm{d}t' \tag{19}$$

where $m$ indicates the radius $r_m$. The rate of shear over the range of time $t_u \leq t < t_{u+1}$ is given by

$$\dot{\gamma}_{um} = \frac{g_{u+1,m} - g_{um}}{\Delta} \tag{20}$$

We wish to express the stress $\sigma_{nm}$ at $t=t_n$ and $r=r_m$ in terms of the quantities $g_{um}$. The relative strain of Eq. (12) at $r=r_m$ can be written as

$$\gamma_m(t, t') = g_{nm} - g_{um} - \dot{\gamma}_{um} s\Delta \tag{21}$$

if $t_u \leq t' < t_{u+1}$. By employing Eq. (21) in Eq. (11) and changing the variable $t'$ to $s$, one can carry out the integral analytically over every $\Delta$ period. Thus the shear stress $\sigma_{nm}$ is expressed in terms of $g_{um}(u \leq n)$. The calculation is lengthy but trivial. We do not show the result here. Likewise the shear stress $\sigma_{n+1,m}$ is expressed in terms of $g_{um}(u \leq n+1)$.

Here we assume that the rate of shear changes only slightly at $t=t_n$, *i.e.*, the quantity $\varepsilon_m$ is small if we write

$$\dot{\gamma}_{nm} = \dot{\gamma}_{n-1,m} + \varepsilon_m \tag{22}$$

The stress $\sigma_{n+1,m}$ is expressed in terms of $g_{um}(u \leq n)$ and $\varepsilon_m$. Expanding $\sigma_{n+1,m}$ in terms of $\varepsilon_m$, we obtain

$$\sigma_{n+1,m} - \sigma_{nm} = a_{nm} + \varepsilon_m b_{nm} + 0(\varepsilon_m^2) \tag{23}$$

where $a_{nm}$ and $b_{nm}$ are known functions of $g_{um}(u \leq n)$. According to the stress equation of equilibrium (6), the quantity $r_m^2 \sigma_{nm}$ should not vary with the suffix $m$. Hence the quantity $r_m^2(\sigma_{n+1,m} - \sigma_{nm})$ is independent of $m$ and we obtain

$$r_m^2(a_{nm} + \varepsilon_m b_{nm}) = c_n \tag{24}$$

where $c_n$ is an unknown quantity independent of $m$. The boundary condition (10) at time $t_{n+1}$ may be written as

$$\sum_m \frac{\varepsilon_m}{r_m} = 0 \tag{25}$$

provided that the strain $g_{nm}$ at time $t_n$ satisfies the boundary condition

$$\sum_m \frac{g_{nm}}{r_m} = \Omega t_n \tag{26}$$

Equations (24) and (25) can be regarded as a set of linear simultaneous equations to be solved for $M+2$ quantities, $\varepsilon_m$ $(1 \leq m \leq M+1)$ and $c_n$. If one knows the right distribution of the rate of shear up to the time $t_n$, then one can calculate that at $t_{n+1}$ and the procedure can be repeated for the succeeding times.

At the very beginning of the shear flow, the distribution of the rate of shear is well approximated by Eq. (2), which is applicable to slowly varying flow of linearly viscoelastic materials. The statement is true for materials whose nonlinear behavior is described by strain-dependent constitutive equations such as Eq. (13). For these materials the rheological behavior at the very beginning of flow is not affected by the rate of shear because the amount of strain is small at short times; in the case of Eq. (14) for example, the nonlinear effect may not be of importance when the product $\alpha\gamma$ is much smaller than unity, *i.e.*, at times smaller than say $10^{-2}/\alpha\dot{\gamma}$ at the beginning of flow.

**Numerical Calculations**

Numerical calculations were performed with FACOM 230–48 of the Institute for Chemical Research, Kyoto University, for the following cases;
*constitutive model*: two BKZ models described by Eqs.(15a) and (15b);
*geometry*: Two different gaps, $(R_o-R_i)/R_c=0.1$ (narrow gap) and 0.2 (wide gap), were examined, where $R_c=(R_o+R_i)/2$;
*rate of shear*: calculations were performed at rates of shear corresponding approximately to $\eta/\eta^0=0.5$, 0.2, and 0.1 at the center of the gap, $r=R_c$, for every combination of the model and the gap.

The cylindrical gap $(R_i, R_o)$ was divided into up to 32 shells and the initial condition was given by

$$g_{1m} = 0 \tag{27a}$$

$$g_{2m} = \frac{2\Omega\Delta}{r_m^2(R_i^{-2}-R_o^{-2})} \tag{27b}$$

*i.e.*, the rate of shear was assumed to be given by Eq. (2) for the first $\Delta$ interval. Then $\varepsilon_m$ and hence $g_{nm}$, was calculated step by step for the succeeding points of each $\Delta$ interval.

Preliminary calculations showed that the result was rather insensitive to the number of division $M$ of the gap $(R_i, R_o)$: the $M$ value of 16 led to less than 1 % deviation from the cases of larger $M$ even in the case of the wide gap. The result did not depend on the quantity $\Delta$ when $\Delta$ was smaller than $10^{-2}/\alpha\dot{\gamma}$. The value $10^{-2}/\alpha\dot{\gamma}$ is larger than the stress-equilibrating time $t_{eq}$ as discussed below Eq. (8) even at the maximum rate of shear of the present calculation if the relaxation time $\tau_1$ is sufficiently large, *i.e.*, $\tau_1 > 10$s. The following results may be exact to within 2 %. The rate of shear is given in a reduced form $\dot{\gamma}\tau_1$ as a function of a reduced time $t/\tau_1$ and a reduced distance $r/R_c$. The shear stress at $r=R_c$ is given in a reduced form $\sigma/\tau_1 G_1\dot{\gamma}_\infty$, where $\dot{\gamma}_\infty$ is the rate of shear in steady state at $r=R_c$.

## RESULTS AND DISCUSSION

### Time Dependence of Rate of Shear

Figures 5 through 7 show how the rate of shear changes with time at fixed points for the case of the constitutive model I and the wide gap geometry. The reduced

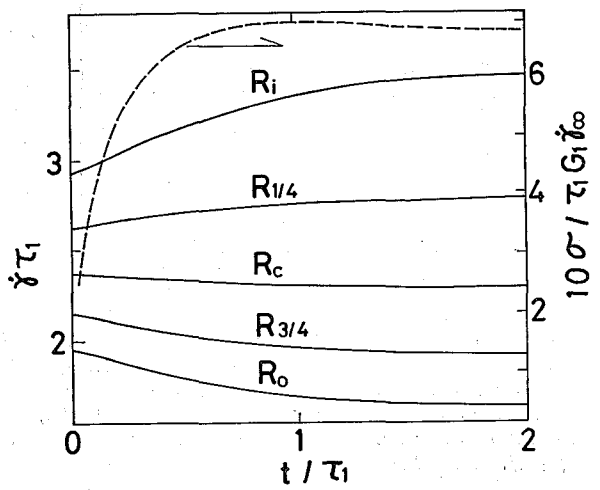


Fig. 5. Calculated results for combination of model I and wide gap geometry, $(R_o-R_i)/R_c=0.2$, at relatively low rate of rotation, corresponding to $\eta/\eta^0\simeq 0.5$ at $r=R_c$. Solid lines indicate reduced rates of shear $\dot{\gamma}\tau_1$ at various radii; $r/R_c=0.90$ ($R_i$), 0.95 ($R_{1/4}$), 1.00 ($R_c$), 1.05 ($R_{3/4}$), and 1.10 ($R_o$) from top to bottom. Dashed line indicates reduced shear stress $\sigma/\tau_1 G_1\dot{\gamma}_\infty$ at $r=R_c$, where $\dot{\gamma}_\infty$ is rate of shear in steady state.

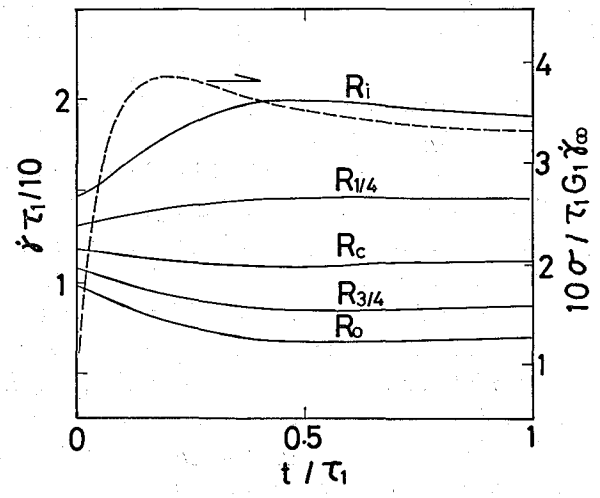


Fig. 6. Calculated results for combination of model I and wide gap geometry, $(R_o-R_i)/R_c=0.2$, for moderate rate of rotation, corresponding to $\eta/\eta^0\simeq 0.2$ at $r=R_c$. Solid lines indicate reduced rates of shear $\dot{\gamma}\tau_1$ at various radii; $r/R_c=0.90$, 0.95, 1.00, 1.05, and 1.10 from top to bottom. Dashed line indicates reduced shear stress $\sigma/\tau_1 G_1\dot{\gamma}_\infty$ at $r=R_c$.

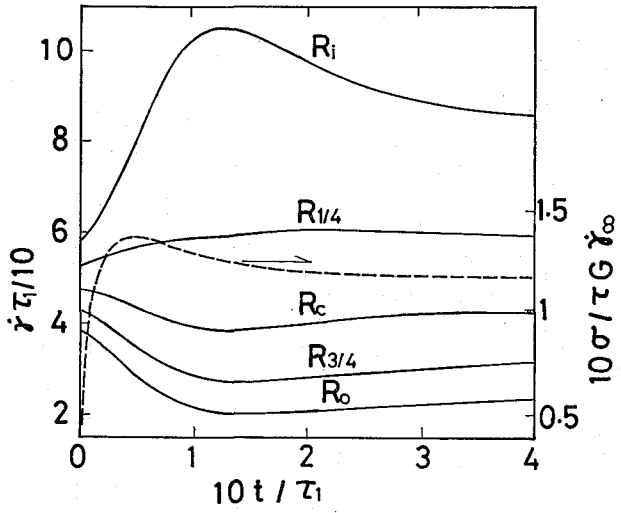


Fig. 7. Calculated results for combination of model I and wide gap geometry, $(R_o-R_i)/R_c=0.2$, for high rate of rotation, corresponding to $\eta/\eta^0\simeq 0.1$ at $r=R_c$. Solid lines indicate reduced rates of shear $\dot{\gamma}\tau_1$ at various radii; $r/R_c=0.90$, 0.95, 1.00, 1.05, and 1.10 from top to bottom. Dashed line indicates reduced shear stress $\sigma/\tau_1 G_1\dot{\gamma}_\infty$ at $r=R_c$.

rates of shear $\dot{\gamma}\tau_1$ at five points separated by the same distance along the radius are plotted against the reduced time $t/\tau_1$; $R_{1/4}$ and $R_{3/4}$ correspond to $R_i+(R_o-R_i)/4$ and $R_i+3(R_o-R_i)/4$, respectively. The reduced shear stress $\sigma/\tau_1 G_1\dot{\gamma}_\infty$ at the center of gap $r=R_c$ is also shown.

In Fig. 5 the rate of shear varies monotonously with time at each point: The rates of shear at $R_i$ and $R_{1/4}$ increase and those at $r\geq R_c$ decrease with time. The rates of shear at $t/\tau_1=2$ are in close agreement with those evaluated from Eq. (4) with $n=0.31$ obtained from Fig. 2. The decrease of $\dot{\gamma}$ at $R_c$ is small, and 4 % in this case. It may be expected from Fig. 5 that the rate of shear is almost independent of time at a point in the range $R_{1/4}<r<R_c$.

The same qualitative features as summerized in Fig. 5 are obtained for all the combinations of constitutive models I and II and the geometries of wide and narrow gaps when the rate of shear is relatively low, *i.e.*, when the ratio $\eta/\eta^0$ at $R_c$ is approximately 0.5. The difference due to the model is that the variation of $\dot{\gamma}$ is larger for the model II than for the model I. The difference is attributable to the fact that the value of $n$ for the model II is smaller than that for the model I at the rate of shear corresponding to $\eta/\eta^0=0.5$. The rates of shear at $R_i$ and $R_o$ for the narrow gap system, naturally varying to a smaller extent than those for the wide gap system, are roughly equal to the rates of shear at $R_{1/4}$ and $R_{3/4}$, respectively, for the wide gap system. The rate of shear at $R_c$ for the narrow gap system varies only slightly; in the case of model I, for example, it decreases by 1 % with time as compared with 4 % for the wide gap system.

As the rotation velocity increases, the rate of shear at each point becomes to exhibit either a maximum or a minimum depending on whether the radius $r$ is smaller

or larger, respectively, than a certain critical value, which is slightly smaller than $R_c$. The maxima and minima are located at the time which is given by the 2.5-3 times of that corresponding to the maximum of the shear stress. The rate of shear at $R_c$ becomes to exhibit a minimum of a considerable depth; the values of $\dot{\gamma}$ at the minima of Figs. 6 and 7 are respectively 9 and 20 % lower than the initial values. The corresponding figures for the narrow gap system are 2.2 and 5 %, respectively, when the initial values of $\dot{\gamma}$ are approximately equal to those of Figs. 6 and 7. The variation of $\dot{\gamma}$ at $R_c$ is suppressed largely with decreasing width of the gap. It is likely that the rate of shear scarcely varies at a certain radius slightly smaller than $R_c$. We will discuss on the significance of this fact later.

From the results given above, one may note that the rate of shear in the wide gap system varies to a greater degree with time than that in the narrow gap system does. One may also see that the time dependence of $\dot{\gamma}$ for the model II is stronger than that of the model I is. Figure 8 shows the result obtained for the combination

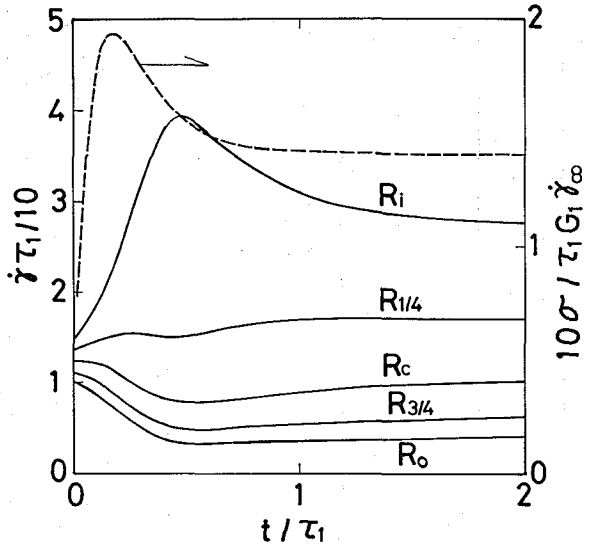


Fig. 8. Calculated results for combination of model II and wide gap geometry, $(R_o-R_i)/R_c=0.2$, for high rate of rotation, corresponding to $\eta/\eta^0=0.1$ at $r=R_c$. Solid lines indicate reduced rates of shear $\gamma\tau_1$ at various radii; $r/R_c=0.90$, 0.95, 1.00, 1.05, and 1.10 from top to bottom. Dashed line indicates reduced shear stress $\sigma/\tau_1 G_1\gamma_\infty$ at $r=R_c$.

of the model II and the wide gap at the rotation velocity approximately corresponding to $\eta/\eta^0=0.1$ at $R_c$. This figure represents the result in which the rates of shear varied to the highest degree and in the most complicated manner in the present calculation. One may note the high maximum value of $\dot{\gamma}$ at $R_i$ and the low minimum at $R_o$. The minimum value of $\dot{\gamma}$ at $R_c$ is smaller than the initial value by about 40 %. The rate of shear at $R_{1/4}$ passes over two maxima and one minimum. This type of oscillatory behavior is not observed in any other case of the present calculations.

**Distribution of Rate of Shear**

Figures 9 and 10 show the distribution of rate of shear at fixed times for the constitutive models I and II, respectively. The left panels show the results for the narrow gap geometry and the right panels for the wide gap. The rate of shear is plotted against the radius with double-logarithmic scales so that Eqs.(2) and (4) are represented by straight lines.

Except for the case of the model II combined with the wide gap geometry, the results for the longest time, $t/\tau_1=2$, of calculation are in good agreement with those

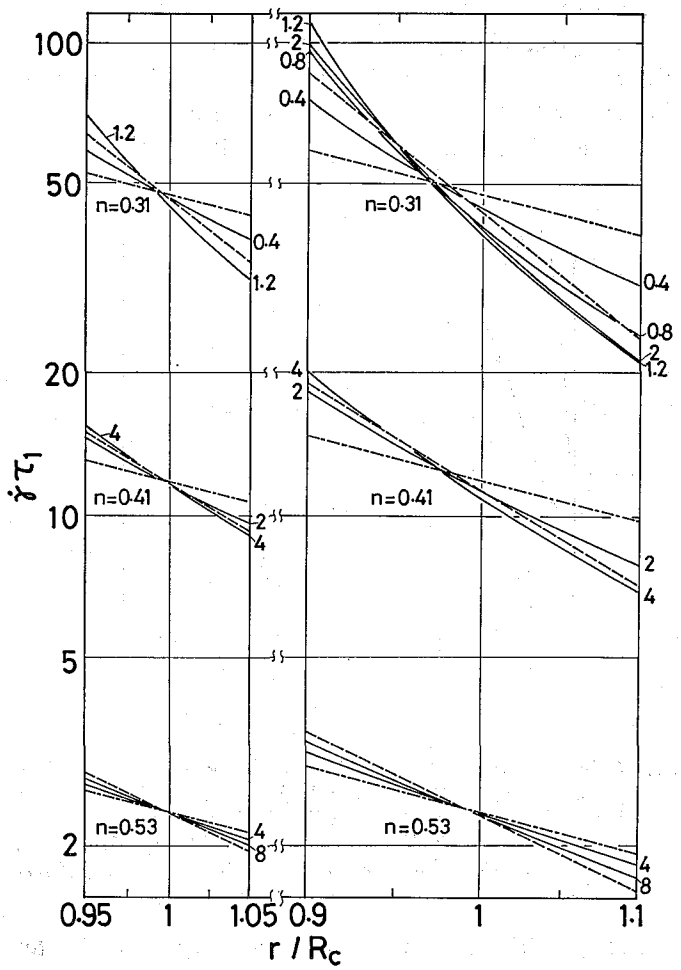


Fig. 9. Results for distribution of rate of shear at various times for model I. Left panel gives results for narrow gap geometry and right panel for wide gap. Reduced rate of shear $\gamma\tau_1$ is plotted against reduced radius $r/R_c$ with double logarithmic scales for three rotation velocities on each panel. Chain lines and broken lines are due to Eqs. (2) and (4), respectively. Values of $n$ indicated were evaluated from Fig. 2 at $\gamma\tau_1$ values corresponding to steady state at $r=R_c$. Figure attached to each solid line indicates value of $10t/\tau_1$. Results for $t/\tau_1=2$ lie to within $\pm 2$ % of dashed lines for all cases.

obtained from Eq. (4) and the values of $n$ evaluated from Fig. 2. The noticeable disagreement on the right panel of Fig. 10 between the results for $t/\tau_1=2$ and those from Eq.(4) is due to the approximate nature of Eq.(4) applied to the system represented by Fig. 2. For the combination of model II and wide gap geometry, the rate of shear in steady state varies largely over the cylindrical gap, and it is not a very good approximation to represent the rheological behavior with a single value of $n$ over the wide range of rate of shear. The result for $t/\tau_1=2$ is proved to be in accord with the stress equation of equilibrium (6) if the value of $n$ correspond-

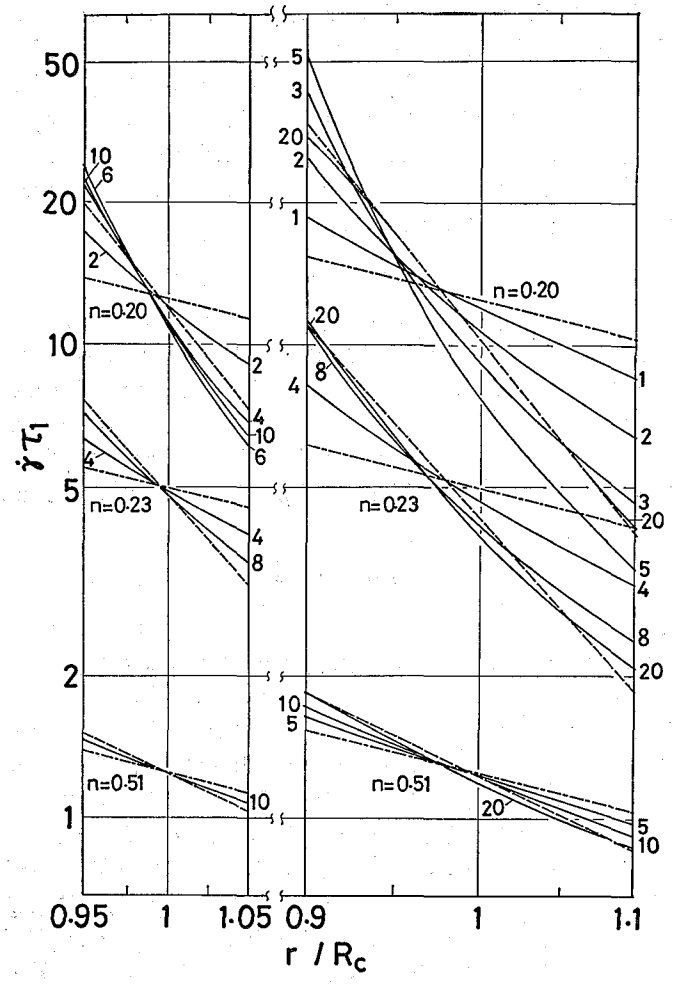


Fig. 10. Results for distribution of rate of shear at various times for model II. Left panel gives results for narrow gap geometry and right panel for wide gap. Reduced rate of shear $\dot{\gamma}\tau_1$ is plotted against reduced radius $r/R_c$ with double logarithmic scales for three rotation velocities on each panel. Chain lines and broken lines are due to Eqs. (2) and (4), respectively. Values of $n$ indicated were evaluated from Fig. 2 at $\dot{\gamma}\tau_1$ values corresponding to steady state at $r=R_c$. Figure attached to each solid line indicates value of $10\ t/\tau_1$. Results for $t/\tau_1=2$ lie to within $\pm 3$ % of dashed lines for left panel.

ing to the calculated rate of shear at each point is determined from $n=d\ln(\dot{\gamma}\eta)/d\ln\dot{\gamma}$. It may be noted here that Eq. (4) based on the power law approximation gives a sufficiently precise values, say to within 10 %, for use in viscosity measurements.

A rough observation of Figs. 9 and 10 may be sufficient to see that the variation of the rate of shear at $R_c$ is reduced rapidly with decreasing gap width and that the rate of shear at a certain point in the range $R_{1/4}<r<R_c$ approximately stays constant when the gap width is small. These two features are important in justifying the use of the coaxial cylinder rheometer for the measurements of time-dependent rheological functions; the former is related to the optical measurements in which the light ordinarily is led along the axis at $r\simeq R_c$ and the latter to the stress measurement as explained in the following section. When the gap width is large and the material exhibits marked nonlinearity, the rate of shear at $R_c$ varies considerably with time and the rate of shear is not controllable, *i.e.*, it does not stay constant in the present case, at any point of the material. Thus the wide gap system may be used for time-dependent measurements only at very low rates of shear where the nonlinear behavior of the material is not very marked.

**Practical Use for Time-Dependent Measurements**

It is easily shown that the coaxial cylinder rheometer can be employed for measuring the time-dependent shear stress at the start of steady shear flow as far as the rate of shear stays constant at least at one point. Suppose the rate of shear has a constant value $\dot{\gamma}_s$ at a certain point, $r=R_s$, irrespective of the time. The torque exerted on the inner cylinder can be measured in ordinary coaxial cylinder rheometers. The torque gives the shear stress $\sigma_i(t)$ at $r=R_i$. According to Eq. (6), one obtains a relation

$$\sigma_i R_i^2 = \sigma_s R_s^2 \tag{28}$$

where $\sigma_s(t)$ is the shear stress at $r=R_s$. Thus one obtains the shear stress $\sigma_s(t)$ corresponding to the constant rate of shear $\dot{\gamma}_s$ by measuring the shear stress $\sigma_i(t)$ corresponding to the time-dependent rate of shear at $r=R_i$.

As noted earlier, the rate of shear at one point scarcely depends on time in the case of the narrow gap system in the present calculations. The point lies in the range $R_{1/4}<r<R_c$ as seen in Figs. 9 and 10. The condition that the rate of shear stays constant at the point is fulfilled to within 10 % for either of the constitutive models I and II in the narrow gap system. It is likely that the condition may be fulfilled to within few per cent if the gap is made smaller, say $(R_o-R_i)/R_c=0.05$, which is not unusual for a practical rheometer. This criterion may be applied to real polymeric liquids, most of which exhibit non-Newtonian effect to the degree somewhere between the two models of the present calculation. One can evaluate the radius $R_s$ by equating Eqs. (2) and (4),

$$\frac{R_s}{R_c} \simeq 1-\frac{5+\dfrac{2}{n}}{24}\left(\frac{R_o-R_i}{R_c}\right)^2 \qquad (n\neq 1) \tag{29}$$

where $n=d\ln(\dot{\gamma}\eta)/d\ln\dot{\gamma}$. The rate of shear $\dot{\gamma}_s$ is obtained from Eq. (2) by putting

$r=R_s$. Needless to say, one can use Eq. (2) and apply the rheometer in an ordinary manner to any slowly varying flow if $n$ is close to unity.

## REFERENCES

(1) See for example, K. Walters, "Rheometry", Chapman and Hall, London, 1975, Chapter 4.
(2) I.M. Krieger and S.H. Maron, *J. Appl. Phys.*, **25**, 72 (1954).
(3) H. Markovitz, *J. Appl. Phys.*, **23**, 1070 (1952).
(4) See for example, H.J. Bixler and O.J. Sweeting, "The Science and Technology of Polymer Films", vol.2, ed. by O.J. Sweeting, Wiley, New York, 1971.
(5) B. Bernstein, E.A. Kearsley, and L.J. Zapas, *Trans. Soc. Rheol.*, **7**, 391 (1963); **9**, 27 (1965).
(6) See for example, K. Osaki, *Proc. 7th Intern. Congr. Rheology*, C. Klason and J. Kubat, ed., Gothenberg, 1976, p. 104; K. Osaki, *J. Soc. Rheol., Japan*, **4**, 163 (1977).
(7) M.H. Wagner, *J. Non-Newtonian Fluid Mech.*, **4**, 39 (1978).
(8) H.M. Laun, *Rheol. Acta*, **17**, 1 (1978).